BULLETIN OF THE EARTHQUAKE
RESEARCH INSTITUTE
UNIVERSITY OF TOKYO
Vol. 59 (1984) pp. 441-465

Hypocenter Distribution in the Japan Trench Region, off Sanriku, Northeast Japan, Determined by an Ocean-Bottom Seismometer Array Observation

Shozaburo NAGUMO, Junzo KASAHARA and Sadayuki KORESAWA

Earthquake Research Institute, University of Tokyo

(Received October 31, 1984)

Abstract

An OBS array observation (seven stations and one month) was performed in June and July, 1981 off-Sanriku, Japan Trench region, Northeast Japan. The array covered the area of both the island-arc side and the ocean basin side of the trench axis. In order to improve the resolution capability of focal depth estimation, we developed a new earthquake location algorithm, which is characterized by a ray initializer technique for the three-dimensional heterogeneous velocity structure, an addition of the origin time constraint in the least-square-iteration procedure, and another addition of an examining procedure for the effect of the initial trial-focal-depth. Three distinct groups were revealed in the hypocenter distribution in the Japan Trench region. (1) One group is a long and narrow zonal distribution along the bathymetric contour of a depth of about 6 km in the outer-slope region. The depths of these earthquakes are shallow within the ocean crust. They appear to correspond to the graben structures in this region representing the bending motion of the ocean crust. (2) Another group is the earthquakes in clusters near the trench axis in the outer-slope region. The depths of these earthquakes extend deep into the uppermost mantle beneath the Moho discontinuity from the shallow crust along a nearly vertical plane representing a lithospheric faulting motion. This place corresponds to the locatin of the main shock of the 1933 large off-Sanriku earthquake. This seismicity appears to be associated with the subsidence and a sharp bending deformation of the subducting ocean crust under the inner-slope region after crossing the trech axis. (3) The third group is the swarm earthquakes in the inner-slope region at a water depth of 2-3 km. The depths of these earthquakes are nearly at the interface between the overlying landside rock mass and the underlying ocean crust. This seismic activity would represent either a slip or a thrust faulting motion along the interface.

1. Introduction

Accurate depth distribution of hypocenters in the deep-sea trench region is essential for clarifying the configuration and present-day motion of the subducting oceanic plate. Such accurate depth determination can only be achieved by the data set of P- and S-wave arrival times observed at array stations right above the hypocenters. Covering such a region in the Japan Trench axis, an ocean-bottom seismometer (OBS) array observation was performed in the summer (June-July) of 1981 off Sanriku, Northeast Japan. The OBS array, consisting of seven OBS's stations covered both the ocean basin side and the island-arc side of the trench axis.

As preliminarily reprorted (KASAHARA et al., 1982, hereafter refer to Paper I), we found there several remarkable features of the epicenter distribution; (1) a long linear trend of epicenter distribution in the outer-slope region of the Japan Trench along the bathymetric contour at a depth of about 6 km, (2) a cluster of epicenters near the trench axis in the outer-slope region, whose place corresponds to the hypocenter of the main shock of the 1933 Sanriku earthquake (M=8.3), (3) a particular swarm earthquake activity in the inner-slope region. These hypocenters were determined by using the hypocenter location program HYPO71 (LEE and LAHR, 1975). Although the epicenter locations were good, there remained uncertainty about the reliability of the focal depth. Therefore, we have attempted to improve the earthquake location algorithms for obtaining high resolution and high reliability of the focal depth estimation.

Improvement of the accuracy of the hypocenter determination in the deep-sea trench region is classical as well as an unfinished problem. By now, many studies have been made on this problem; for example, one by improving the earthquake location algorithms (ICHIKAWA, 1978b, 1979; ENGDAHL and LEE, 1976; ENGDAHL et al., 1982), and another by conducting OBS array observations (NAGUMO et al., 1970, 1976; FROHLICH et al., 1982; HIRATA et al., 1983). Although the accuracy of epicenter determination has been greatly improved by the use of proper travel-time tables, ray tracing technique, and OBS data in the hypocenter region, the accuracy of focal depth determination has still remained unsatisfactory.

The improvements we have made on this problem are as follows. First, in order to reduce the error due to three-dimensional hetrogeneous seismic velocity structure, which is inherent in the deep-sea trench region, the technique of ray initializer (THURBER and ELLWORTH, 1980) was introduced in the earthquake location program HYPO71 by NISHI (1982). Although the O-C residuals of the hypocenter determination were greatly

improved, the focal depth was still dependent on the depth of the initial trial-hypocenter in the least-square iterative procedure. Next, we proceeded to improve the earthquake location algorithm itself. We examined effects of the initial trial-origin-time and initial focal depth, and understood that the depth solution generally possesses dual values, one is shallower, the other is deeper with respect to the major refraction velocity discontinuity (SUGIMOTO, 1983). Similar dual value property has already been noticed by LILWALL et al. (1978), DUSCHENS et al. (1983), and FROHLICH et al. (1982).

Following these studies, we developed in this paper a new algorithm which utilizes (1) the technique of the ray initializer for treating three-dimensional seismic wave velocity structure, (2) the addition of a constraint on the origin time in the least-square optimization procedure, and (3) another addition of an examining procedure for the effect of the initial trial-focal depth. The new algorithm resulted in high capability of depth resolution and revealed close relations between the hypocenter distribution and the present-day tectonic movements of the subducting oceanic plate.

Thus the purpose of this paper is, firstly, to present a new earthquake location algorithm, and secondly, to present results which revealed remarkable features of the hypocenter distribution in the Japan Trench region. Since descriptions of the instruments and the station data are given in Paper I, we do not repeat them here.

2. Method of hypocenter determination

In this section, first we will list the major problems which we encounter in the course of the hypocenter location in the deep-sea trench region, and then we will describe how we treated them.

Problems

The major problems which disturb high resolution of hypocenter location in the deep-sea trench region are as follows:

(1) three-dimensional hetrogeneous seismic wave velocity structure,
(2) effect of soft sediment layer beneath sea-floor in which S-wave velocity is extremely low,
(3) treatment of sea-bottom topography and station depth,
(4) estimation of origin time,
(5) treatment of dual-valued solutions for the focal depth.

Items (1) and (3) affect the accuracy of travel-time calculation, and items (4) and (5) affect the optimization algorithm itself.

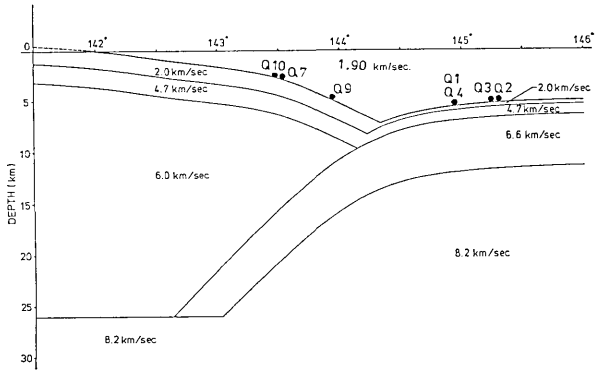

Fig. 1. Three-dimensional P-wave velocity structure in the Japan Trench region used in the hypocenter computation (after NISHI, 1982). Solid circles: OBS stations.

Three-dimensional hetrogeneous structure

As is well known, systematic deviations of hypocenter location occur in the deep-sea trench region (for example, ICHIKAWA, 1978a; ENGDAHL et al., 1982). This is caused by the velocity structure associated with deep seismic zone. In order to reduce such deviation, three-dimensional ray tracing technique has been used for hypocenter determination (for example, JACOB, 1970; ENGDAHL and LEE, 1976; JULIAN and GUBBINS, 1977). However, because of large computation time, it has not yet been used for the routine hypocenter location program. In order to reduce this computation times, THURBER and ELLWORTH (1980) has shown that the ray initializer approximation is almost accurate enough for calculating travel-times, and this technique was introduced in the hypocenter location program HYPO71 by NISHI (1982). In this paper we utilized a part of his ray initializer program, which computes three-dimensional P- and S-wave velocity structures, travel-times and their derivatives. Because of the memory size of our computer (HARRIS 80), we limited the total number of grid points of three-dimensional velocity structure to 75,020 points. The areas of computation are from 141°30′E to 145°30′E, and from 38°00′N to 41°00′N, with the mesh interval of 5′. The total number of the flat-layers of slowness average is 44. We used the same three-dimensional velocity structures as was used by NISHI (1982) as shown in Fig. 1.

Sea-bottom topography and station depth

We treated the station depth exactly. Namely, we computed travel-time from the source to the station which is located at a given depth. When OBS array covers both the landward side (continental slope) and

oceanward side (outer-slope) of the trench axis, the differences of elevation among OBS stations amount to more than 4 km. In such case the slowness average which is used in the ray initializer approximation is affected by the sea-water and causes inadequate travel-times to the stations in the landward side. In order to avoid such errors of travel times, we replaced the sea-water layer by a layer of P-wave velocity of 1.90 km/sec, which is slightly less than that of the underlying soft sediment layer (in this case 2.00 km/sec). This treatment gives sufficiently accurate travel-times for the stations in the landward side.

Soft sediment layer

As is well known, the top layer beneath the deep ocean floor consists of soft sediments, whose thicknesses are from a hundred to several hundred meters, and its S-wave velocity is extremely low, as low as from several tens to several hundreds meters/sec (for example, HAMILTON, 1976; NAGUMO et al., 1980). Because of such a low S-wave velocity, the arrival time of S-wave is delayed within the soft sediments and this results in a large S–P time. For example, in a case where the soft sediments layer has a thickness 500 m, where P- and S-wave velocities are 2.0 km/sec and 0.4 km/sec respectively, the S–P time within the layer amounts to 1.00 second. Since we use S–P time for estimating the origin time, if such a delay time is not properly corrected, it will mislead the origin time estimation to be earlier than it actually is. In order to correct the delay of S-wave arrival time, we used the same correction as used in the previous paper (Paper I), namely we subtructed observed PS delay time from the S-wave arrival time at each station. The PS delay time is defined by the difference between P arrival time on the vertical component and P-to-S conversion arrival time on the horizontal component.

Origin time

Accurate estimation of origin time is most essential to the depth resolution. It is common in the conventional hypocenter location program such as HYPO71, the origin time is treated as one of the 4 unknown parameters (the origin time and 3 hypocenter coordinates), and is determined simultaneously with hypocenter coordinates in the course of the least-square computation. In such a treatment, it often occurs that the origin time largely differs from the true value.

Since origin time can be determined by P and S–P time readings independently from hypocenter coordinates, several techniques have been developed for special treatment of origin time. JAMES et al. (1969) deve-

loped the 'three-parameter technique'. Shibuya (personal communication) developed a program which allows both 'three-parameter' calculation and conventional 'four-parameter' calculation. ICHIKAWA (1978b) developed a technique which imposes special constraints on the initial origin time. In this paper, we used such algorithm as follows. First we compute the origin time from P and P–S times, and then, by fixing this origin time, we compute the hypocenter coordinates by the least-square-iteration procedure, which is nothing but the 'three-parameter technique' of JAMES et al. (1969). Then, by using this origin time and hypocenter as the initial trial-values, we proceed to the 'four-parameter' least-square-iteration computation. Since the initial trial-values of the four-parameter least-square-iteration procedure have been searched by constraining the origin time, the above procedure could be referred to 'origin time constraining optimization'. In this procedure, since the initial trial-epicenter coordinates are already well located by the 'three-parameter technique', the four-parameter least-square-iteration proceeds mainly between the two parameters, namely between focal depth and origin time.

Dual-valued solution of focal depth

When the epicentral distance is in the range where the first arrivals are refracted waves from a certain refraction horizon, there are generally two focal depths which satisfy the given observed travel-time at a certain station, the one is shallower and the other deeper than the refraction horizon. The ray paths are schematically shown in Fig. 2. Therefore, in many cases where the data are absent at the stations near the hypocenter, it will likely occur that least-square-iteration results in dual solutions. In other words, there are generally two minima in the optimization procedure. For a group of upward refracting rays (A in Fig. 2), the least-square-iteration will find a convergence to a shallow focus. On the other hand,

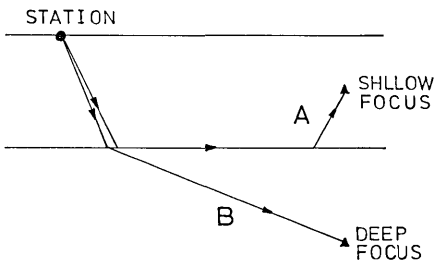

Fig. 2. Explanatory illustration for the existence of dual-valued hypocenter depths which satisfy the least-square minimum value.

for a group of downward-going refracting rays (B in Fig. 2), the least-square-iteration will find a convergence to a deep focus. The identification of the true focal depth from these two solutions can not be made by the examination of travel-time residuals. When we have observation data right above the hypocenter, it can be easy to discriminate the true depth. However, this is not always thec ase. Therefore, in many cases, two different depth solutions are likely to appear according to different initial trial-depths. In principle, the least-square-iteration procedure itself does not discriminate these two minima. Therefore, we proceed to repeat the hypocenter computation several times by giving different initial trial-depths. Moreover, we print out the hypocenter solution at each iteration process so as to examine how the convergence is accomplished. Thus, by examining the effect of the initial trial-depth upon the final convergent depth, we can judge the possible existence of dual-valued solutions and also the optimum selection of the true depth. The initial trial-depths given in the computations this time are 30.0 km and 9.1 km respectively, because the maximum water depth is about 7.5 km at the trench axis and the depth of the Moho discontinuity is about 12 km under the trench axis in this region (LUDWIG et al., 1966).

Flow diagram of hypocenter location algorithm

The conceptional flow diagram of the earthquake location algorithm is shown in Fig. 3. The first step is to compute three-dimensional velocity structure in the form of three-dimensional array data, which will be used in the later stage for computing arrival times, T, and its partial derivatives for each pair of the source and station. The second step is to estimate origin time from P and S-P times by the formula

$$T_O = T_P - kT_{S-P},$$

where

$k = 1/[(V_P/V_S) - 1]$,
T_O: origin time
T_P: P wave arrival time
T_{S-P}: difference of arrival times of P and S waves
V_P, V_S: P and S wave velocities respectively.

The value of k is either assumed or determined by the T_P versus T_{S-P} plot. The third step is the computation of the initial trial-hypocenters which will be used in the succeeding least-square-iteration procedure. Keeping the origin time fixed, the hypocenter is computed by the least-square-iteration procedure. The three-dimensional ray tracing technique

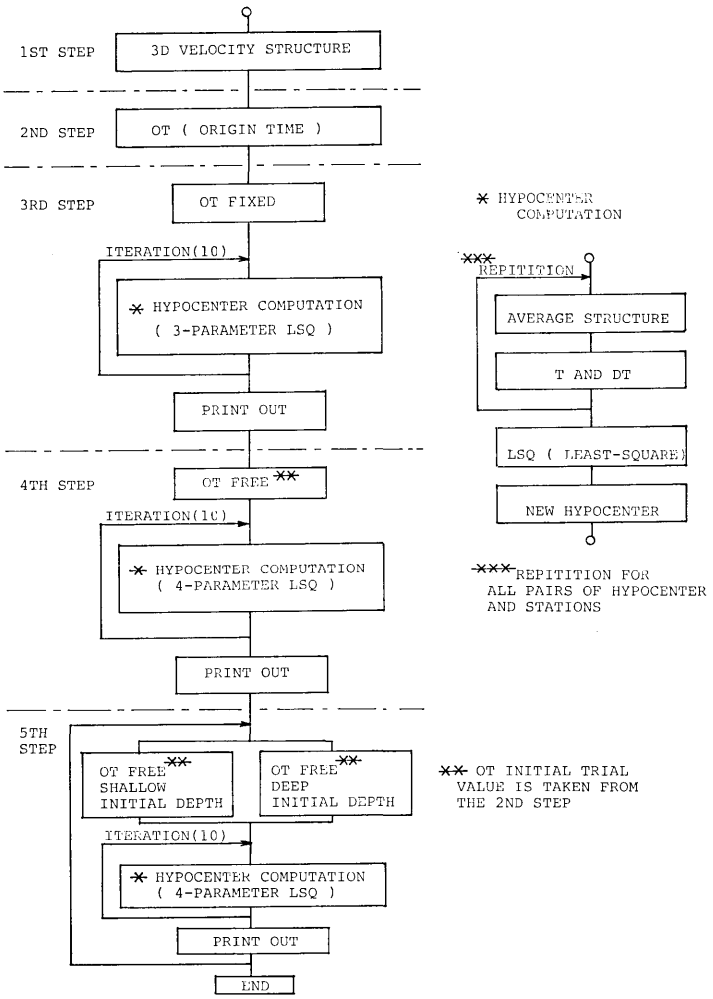

Fig. 3. Conceptional flow diagram of the earthquake location procedure.

is used for computing travel times and their derivatives for each pair of the source and station. The number of iteration is set at 10 times. Generally speaking, epicenters are located well in this step. When the dual-valued solutions exist, the convergence often shows oscillatory nature between shallow and deep focal depths under the constraint of fixed origin time.

The fourth step is the least-square-iteration procedure for the 4 unknown paramaters. In this procedure, we give the origin time obtained in step 2 and the hypocenter coordinates obtained in step 3 as the initial trial-values. In this stage, the optimum value is usually searched mainly in the trade-off between the origin time and the focal depth,

since the epicenter is already located near the optimum value.

The fifth step is the examination of the effect of the initial trial-depth. The least-square-iteration computations are repeated for the given different initial trial-depths. As stated before we repeated the computation for two different depths, the one is shallower (9.1 km) the other is deeper (30 km) than the Moho discontinuity. The initial origin time and the hypocenter coordinates are the same as used in step 4. At each iteration, we print out the process of convergence. Thus we have four different results from steps 3, 4 and 5, which allow us to examine the resolution reliability of the focal depth.

The special features of the algorithm developed in this paper will be summarized as follows: (1) The three-dimensional velocity heterogeneity is treated by ray initializer approximation and resulted in short computation time. (2) By constraining the origin time, the initial trial-hypocenter for the least-square-iteration procedure can be found very close to the optimum value. (3) In the final least-square-iteration procedure, the search for the optimum values proceeds, in many cases, mainly to the trade-off between the origin time and the focal depth. (4) The examinations of the dual-

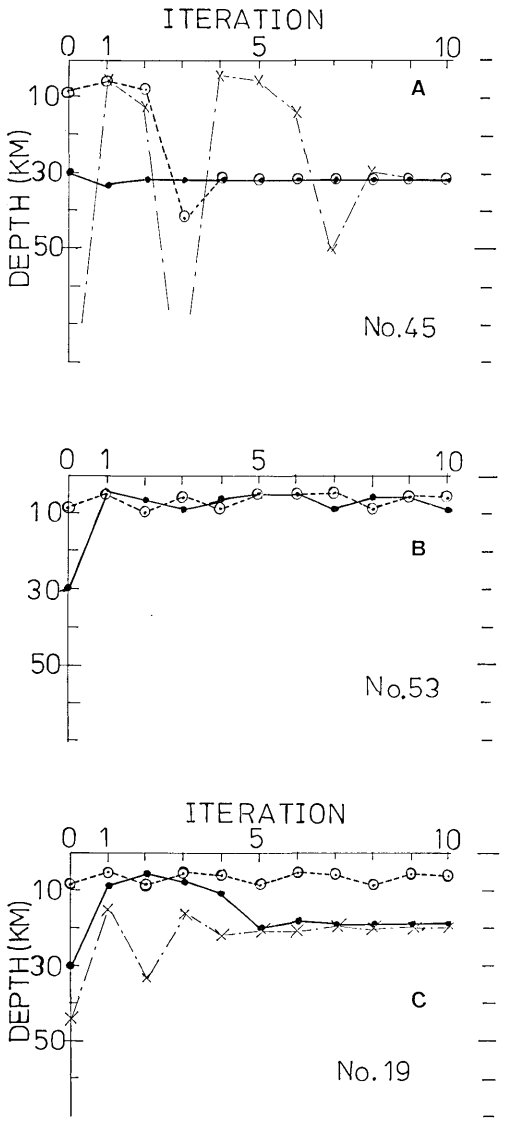

Fig. 4. Examples of the effect of the initial trial depth to the convergence.
The horizontal axis : the number of iteration.
(A) Convergence to a deep focal depth from both shallow and deep initial trial-depths (No. 45 : earthquake number),
(B) Convergence to a shallow focal depth from shallow and deep initial trial-depths (No. 53 : earthquake number),
(C) A shallow initial trial-depth converges to a shallow focal depth, while deep initial trial-depths converge to deep focal depths, showing the presence of double minima in the least-square optimization (No. 19 : earthquake number).

valued solution of focal depth are accomplished by repeating the computation several times for different initial depths. From these features, high resolution of focal depth appear to be accomplished in the deep-sea trench region.

Examples of the examination of initial trial-depth

Examples which show how the resolutin of focal depth is accomplished are shown in Fig. 4. In Fig. 4A and B are shown examples which show that the convergence is achieved to almost the same optimum depth from both shallow and deep initial trial-depths. In such cases as these the convergent depth will be highly reliable. In Fig. 4C is shown that the convergent depths depend on the given initial trial-depth, namely, the shallow initial depth leads to a convergence to a shallow focus, and the deep initial trial depth leads to a convergence to a deep focus. In such a case as this, the selection of the true depth is difficult.

Remarks for least-square optimization

Hypocenter location has been treated as an optimization problem of minimizing the travel-time residuals (for example, LOMNITZ, 1977; LEE and STEWART, 1981). When the seismic wave velocity structure is known, the number of the unknown parameters to be estimated are four, namely, origin time and three hypocenter coordinates. The least-square-iteration procedure is used for obtaining the optimum values. However, the origin time has such property that it can be determined from P- and S-wave arrival times independently from other hypocenter coordinates. This is an additional constraint besides the minimization of the travl-time residuals. Moreover, the minimum value which will be searched by the least-square-iteration procedure is not always unique. In principle, there are two minima in the optimization of the local earthquake location. Thus, the simple least-square-iteration procedure for minimizing the travel-time residuals is not sufficient for the hypocenter location algorithm. A method developed in this paper will be a step towards a better estimation of earthquake hypocenter.

3. Results

Statistics

About 300 earthquakes were registered by an OBS array during the 33 days observation period from June 10 to July 12, 1981. Among these earthquakes, 217 were simultaneously registered by more than four stations.

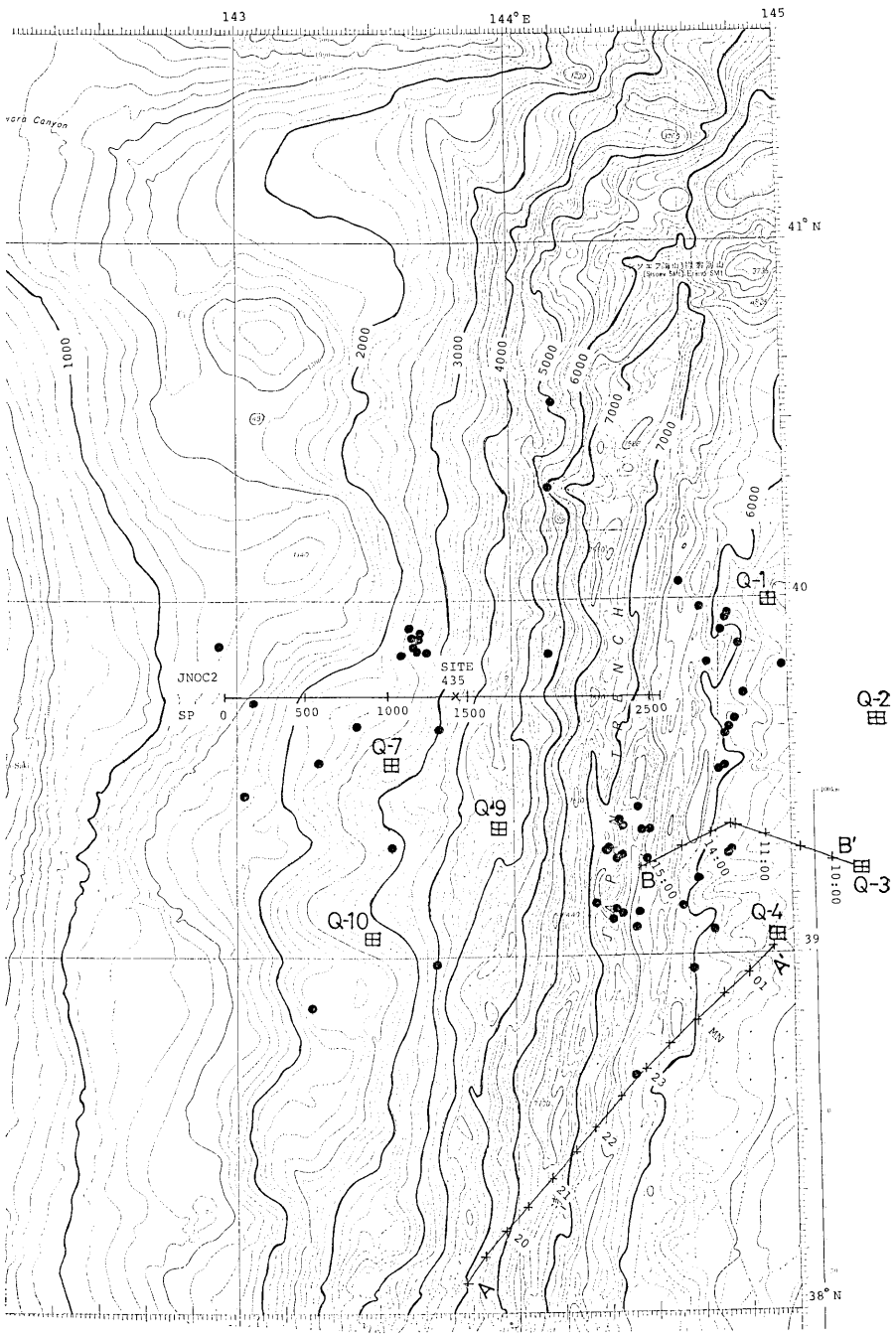

Fig. 5. Epicenter distribution obtained by the new earthquake location procedure. Solid circle: epicenter, Open square with cross: ocean-bottom seismometer station. Bathymetric chart: No. 6321, MARITIME SAFETY AGENCY, 1980.

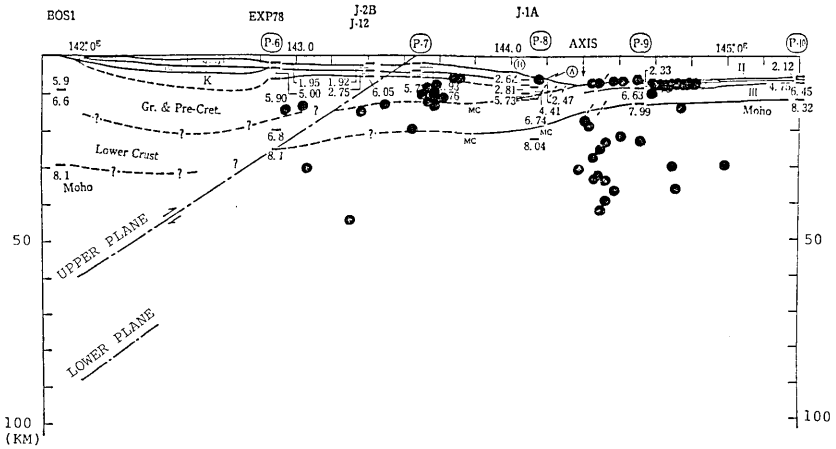

Fig. 6. Depth cross section of the hypocenters obtained by the new earthquake location procedure. Solid circle: hypocenter.

About a half occured in the region in and near the OBS array. About 80 of the earthquakes have been located (Paper I; NISHI, 1982 and SUGIMOTO, 1983).

For these earthquakes, we applied the newly developed earthquake location program described in section 2, and we examined the reliability of the convergence and the depth resolution for each earthquake by plotting the convergence diagram as shown in Fig. 4. From this procedure, we finally obtained hypocenters of 58 earthquakes whose depth resolutions are highly reliable. The epicenter distribution and the focal depth cross section of these earthquakes are shown in Figs. 5, and 6 respectively. The list of these hypocenters is attached in the Appendix.

Epicenter distribution

As reported previously (Paper I), three groups were distinctly identified in the epicenter distribution (Fig. 5); (1) a long and narrow zonal distribution along the bathymetric contour of a depth of about 6 km in the outer-slope region, (2) earthquakes in clusters near to the trench axis in the outer-slope region at almost the same place of the main shock of the 1933 large Sanriku-earthquake (March 2, 1933, M=8.3), and (3) an earthquake swarm in a small area of the inner-slope region whose water depths are from 2 to 3 km.

The epicenter distribution (Fig. 5) obtained in this paper is almost the same as obtained by NISHI (1982), and also it has systematically shifted westward (landward) by about 10 km from those obtained in the previous Paper I. This systematic shift is due to the difference of the assumption

for the velocity structure used in the earthquake location program. In Paper I, the velocity structure assumed was that of a flat-layer, normal ocean crust.

As regards the northeastward extension of this narrow zonal distribution along the 6 km bathymetric contour in the outer-slope region, it appears to exist beyond latitude 40°N. An indication is seen in the previous report (Paper I, Fig. 4). However, because of insufficient accuracy of hypocenter location in this region, being in the out-side of the coverage of the array, the epicenters are omitted in Fig. 5.

In June 3, 22h 50m, 1977, an earthquake swarm activity occurred in the outer-slope region, southeast of the Erimo Seamount (NAGUMO et al., 1978; KASAHARA et al., 1978). Although the accuracy of the epicenters is not sufficient, the epicenter distribution determined by International Seismological Centre and also by OBS data combined with land-based network data showed a linear alignment along the bathymetric contour of a depth of 5.5 km. This swarm activity may correspond to the northeastward extension of the long and narrow zonal distribution found in this paper. Since seismic activity in this region is very high (NAGUMO et al., 1970, 1976; HIRATA et al., 1983), the northeastward extension of the long and narrow zonal seismic activity will be clarified by conducting another OBS array observation in the above region.

The southward extension of this long and narrow zonal distribution was not clear during the present observation period, because of its low seismicity. However, the seismic activity that occurred in March and April of 1983 (JAPAN METEOROLOGICAL AGENCY, 1983; FACULTY OF SCIENCE, TOHOKU UNIVERSITY, 1983) appears to have revealed a southward continuation of this zonal distribution.

From these seismic activities it can be inferred that a long and zonal seismic activity exists along the bathymetric contour of a depth of about 6 km in the outer-slope region of the Japan Trench at least from 38°N to 41°N.

Hypocenter depth distribution

The hypocenters are plotted in Fig. 6 on the profile of a P-wave velocity structure (NAGUMO, 1980), whose vertical exaggeration is about 1 : 1.2. It is quite striking to see that three groups possess different features in the depth distribution. The depths of the earthquakes occurring along the 6 km bathymetric contour are very shallow, within about 3 km from the sea floor, namely, within the upper ocean crust (layer 2 and the upper part of layer 3). On the other hand, the focal depths of the

earthquakes near the trench axis extend from the upper crust into the uppermost mantle beneath the Moho discontinuity, mostly in the range from 15 km to 45 km from the sea-level. The distribution is almost along a nearly vertical plane.

The focal depths of the swarm earthquakes in the inner-slope region are in the range from 10 km to 15 km, and these depths correspond to the depth of the interface between the subducting oceanic plate and the overlying landside rock mass. The configuration of this interface is seen on the multi-channel seismic record section (Fig. 10) (NASU et al., 1979; VON HUENE et al., 1980). The depth resolution described above will be an accomplishment of the newly developed earthquake location algorithm.

4. Discussion

A long and narrow zonal distribution

It is remarkable that the epicenter distribution has shown a long and narrow zonal feature being parallel to the trench axis along the bathymetric contour of a depth of about 6 km in the outer-slope region of the Japan Trench. Hithertoe, the hypocenter distribution in this region was regarded as being scattered in a broad region. Even by OBS observations in the deep-sea trench region, such a narrow zonal distraibution as this has not yet been delineated (FROHLICH et al., 1982; HIRATA et al., 1983). The image of a broadly scattered distribution of epicenters are due to mapping of long-term accumulation of the data, and also due to insufficient accurracy of earthquake location (for example, ICHIKAWA, 1978a, 1979).

The existence of hypocenter concentration in a narrow zone will be a real feature of seismic activity in the deep-sea trench region. This feature was fortunately revealed by an appropriate short-term time window. In the following, we will discuss some tectonic implication of this feature.

Relation to graben structure

The linear trend of a long and narrow zonal distribution of earthquake hypocenters along the 6 km bathymetric contour in the outer-slope region would be associated with the graben structures which exist in the same region. The association is seen in Fig. 5, where epicenters are plotted on the detailed bathymetric chart, on which contour interval is 100 m (MARITIME SAFETY AGENCY, 1980). Profiles of precise depth recorder taken along the traverse during the OBS operation in 1983 are also shown in Figs. 7 and 8. As seen in these figures, there are many graben structures, large and small, in this region. The size of these grabens are full of variety; lengths

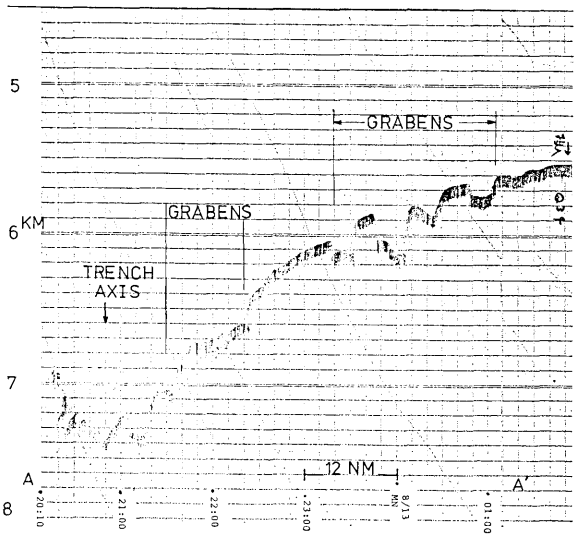

Fig. 7. A PDR (Precise Depth Recorder) profile showing a configuratin of graben structures on the outer-slope of the Japan Trench. The traverse line is AA′ in Fig. 5.

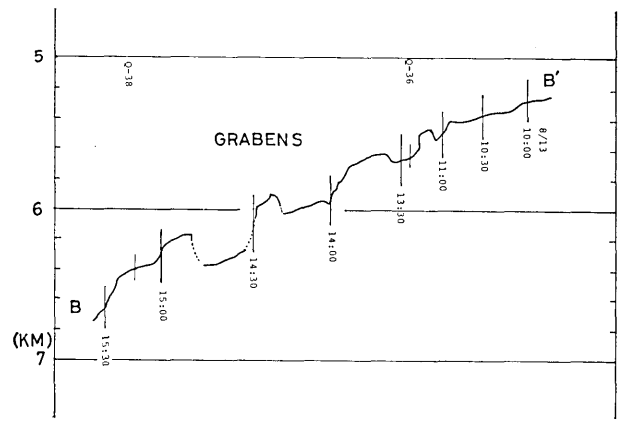

Fig. 8. A line sketch of PDR (Precise Depth Recorder) profile showing a configuration of graben structures on the outer-slope of the Japan Trench. The traverse line is BB′ in Fig. 5, running close to the OBS stations.

of long axis ranging from 10 km to several tens of km, widths from several km to 10 km, and fault steps from 100 m to 300 m (IWABUCHI, 1970 ; LUDWIG et al., 1966). Although the continuation of each graben is not always long, the assembly of these grabens form broad zonal distributions, as a whole, running parallel to the trench axis as seen in Fig. 5.

The earthquakes occurring along the 6 km bathymetric contour cor-

respond to the upper (eastern) margin of the graben structures, where the amount of fault steps are decreasing. The shallow focal depths (within 3 km from the sea floor) seem to imply that these earthquakes occur within the upper ocean crust (layer 2 and the upper part of layer 3). The focal mechanism study of these earthquakes shows that they are the normal fault type with a nearly vertical compressional axis (OCEAN-BOTTOM SEISMOLOGY DIVISION, EARTHQUAKE RESEARCH INSTITUTE, UNIVERSITY OF TOKYO, 1983b), being consistent with a graben forming movement. Since the graben structures are results of bending deformation these features of shallow earthquakes along the 6 km bathymetric contour in the outer-slope region will indicate a present active deformation of the oceanic plate. However, a concentration of the seismic activity along the margin of the bending deformation would imply that the bending deformation of the oceanic plate is not always uniform in the whole region of the deformation, but the oceanic plate could be sharply bent at the transitional zone from the outer-slope region to the ocean basin.

Mantle earthquakes

Another remarkable feature is such that the focal depths of the earthquakes occurring near the trench axis extend to the depths of about 45 km or even more from the sea level. Since the depth of the Moho discontinuity in this region is about 12 km from the sea level (NASU et al., 1979; LUDWIG, et al. 1966), it is evident that these earthquakes occurred within the upper mantle. The distribution of hypocenters along a nearly vertical plane indicates an existence of a fracture plane within the upper mantle. Since the place of these earthquakes corresponds to the hypocenter of the main shock of the 1933 Sanriku Earthquake (March 2, 1933, M=8.3), which is interpreted as fractured through the whole oceanic lithosphere (KANAMORI, 1971), the vertical distribution of seismic activity observed in the present study may be associated with a large fracture plane which exists within the lithoshere.

A possible existence of earthquake foci within the oceanic lithosphere can be seen in the multi-channel seismic record sections. An example is shown in Fig. 9. There are many diffraction sources beneath thet Moho discontinuity. These diffraction sources would be related to faults within the uppermost mantle, and these faults could become foci of micro-earthquakes.

Hithertoe, the focal depths of the earthquakes occurring near the trench axis have been determined deeper than the real ones. This probrem was studied in detail by ICHIKAWA (1979), and he has shown that, by using a

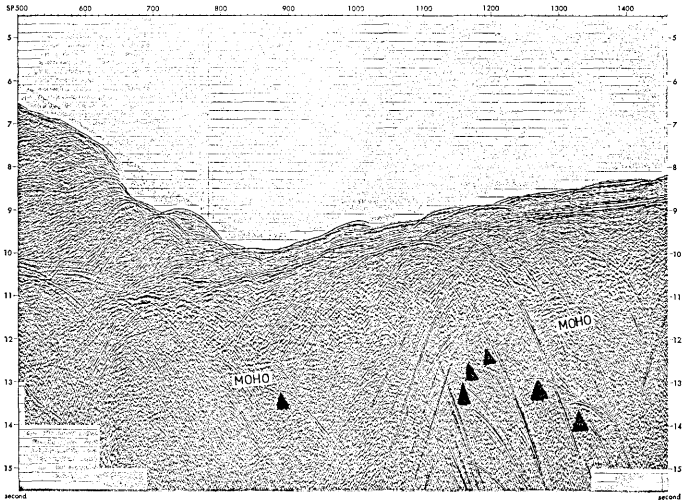

Fig. 9. An example showing the presence of diffraction sources beneath the Moho discontinuity. Solid triangle: diffraction source. The multi-channel seismic record section (time section) is ORI Line 78-4 in the Japan Trench (after NASU *et al.*, 1979).

new travel time table (ICHIKAWA, 1978b), the focal depths of most earthquakes are less than 50 km which formerly were determined as being distributed to a depth of about 100 km. However, he still left questions about whether these earthquakes are even shallower as being limited within the ocean crust or they really occur within the lithosphere beneath the Moho discontinuity. The results obtained in this paper ascertained the latter to be the case.

One of the great concerns in the Japan Trench region is the extension of the lower plane of the dual deep seismic planes towards the trench axis. According to the land observation of the Tohoku University, the lower plane terminates at about longitude 142.5°E at a depth of about 80 km along the E-W traverse in the region of latitude 39°–40°N, and its extension towards the trench axis is obscure because of very low seismicity (HASEGAWA et al., 1978). During the present one month observation period seismic activity along the extension of the lower plane was not observed. However, the finding of the existence of earthquakes within the uppermost mantle near the trench axis certainly indicates that the problem can be solved by conduting a long-term observation in the trench axis region.

Swarm earthquakes in the inner-slope region

Almost all focal depth of the swarm earthquakes occuring in the inner-slope region fell to depths of about 12 km from the sea-level. For-

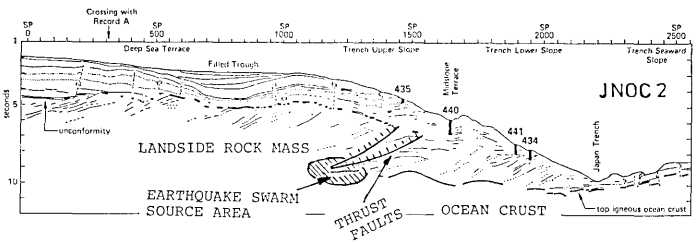

Fig. 10. Projection of the source area of the swarm earthquakes on the line sketch of the multi-channel seismic reflection record section Line JNOC 2, (VON HUENE *et al.*, 1980), with an addition of marks for the thrust faults within the landside rock mass.

tunately, a multi-channel seismic line, upon which the drilling of the IPOD (International Phase of Ocean Drilling) site 435 was conducted (VON HUENE et al., 1980), runs very close to this swarm area. A line sketch of the multi-channel seismic record section is shown in Fig. 10 on which the area of the swarm earthquakes is projected. As seen in this Fig. 10, the place of the swarm earthquakes corresponds to the interface between the subducting ocean crust and the overlying landside rock mass. The place also corresponds to the bases of the large thrust faults which extend upwards to the mid-slope terrace. Since the focal mechanism study of these earthquakes show that they are the thrust fault type (OCEN-BOTTOM SEISMOLOGY DIVISION, EARTHQUAKE RESEARCH INSTITUTE UNIVERSITY OF TOKYO, 1983a), it will be certain that the swarm activity observed this time will be associated with either the slip motion along the interface between the landside rock mass and the underlying oceanic plate or the thrust faulting motion at the base of the faults which extend from the interface into the overlying landside rock mass.

Subsidence and bending of the ocean plate

As KANAMORI (1971) stated, the lithospheric normal faulting is associated with the large scale bending deformation of the oceanic plate in the arc-trench region. However, the presence of a lithospheric fracture plane near the trench axis may indicate that the bending deformation of the oceanic plate is largest there. This feature is seen on the migrated depth section of the multi-channel seismic record sections of the ORI Line 4-3 and Line 4-4 (NASU et al., 1979). As seen in Fig. 11, the configuration of the subducting oceanic plate shows a sharp bending deformation under the inner-slope after crossing the trench axis. And this sharp bending deformation is associated with an additional subsidence of the ocean crust under the trench inner-slope region. We think that this additional subsi-

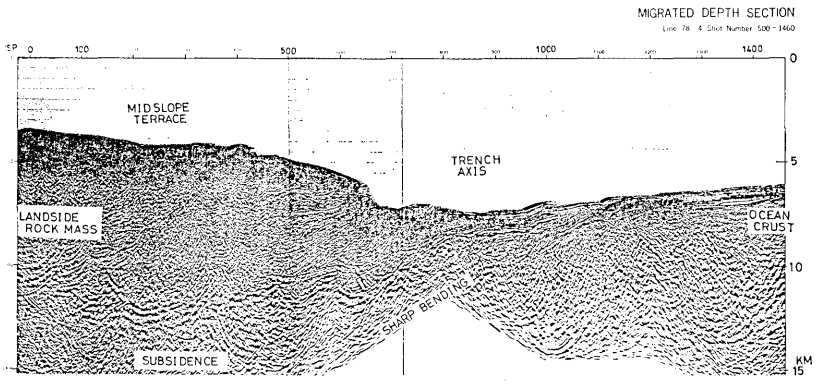

Fig. 11. An example of subsidence and its associated sharp bending of the subducting oceanic crust under the trench inner-slope region after crossing the trench axis. The multi-channel record section is a migrated depth section of the ORI Line 78-4, (after NASU *et al.*, 1979).

dence of the oceanic crust under the trench inner-slope is important for generating the bending deformation of the ocean crust in this region, and that the subsidence is caused by the overlying landside rock mass which acts as an extra load for the underlying ocean crust. This load generates a broad bending deformation of the oceanic plate in the outer slope region. Near the front of the load, that is, near to the trench axis, a sharp bending deformation appears and lithospheric fracture planes are generated there.

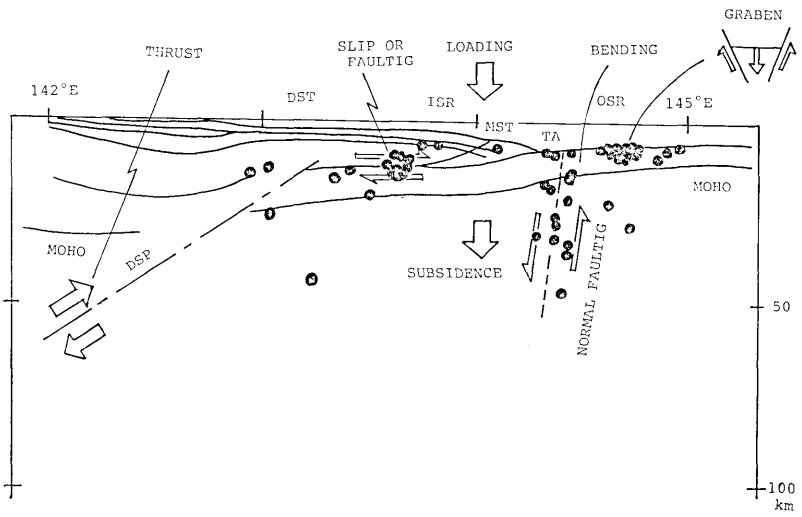

Fig. 12. A schematic illustration of the seismo-tectonic motion in the Japan Trench region. Solid circle : earthquake hypocenter. DST : deep sea terrace ISR : inner-slope region, OSR : outer-slope region, MST : mid-slope terrace, TA : trench axis, DSP : deep seismic plane.

The above mentioned interpretation is schematically illutrasted in Fig. 12. The crust-mantle structure in Fig. 12 is based on multi-channel seismic reflection profiles and seismic refraction studies (NAGUMO, 1980). The vertical exaggeration is about 1 : 1.2, almost the natural scale. A subsidence of the ocean plate occurs under the trench inner-slope, being caused by an extra load due to overlying landside rock mass. This subsidence is associated with a broad bending deformation in the outer-slope region, and a sharp bending deformation occurs near the trench axis, where lithospheric fracture planes are generated. The bending motion generates many graben structures along the surface of the oceanic plate. The ocean plate appears to be sharply bent at the margin of the outer-slope region and is accompanied by a zonal concertration of shallow earthquakes there.

In the trench inner-slope region either a slip motion or a thrust faulting motion occurs along the interface between the landside rock mass and the ocean plate. This motion appears to be associated with the large scale thrust motion along the deep seismic plane.

5. Conclusions

Precise hypocenter distributions have been revealed in the Japan Trench region, Northeast Japan, by an OBS array observation (one month, seven stations in June and July, 1981) using a newly developed high resolution earthquake location algorithm. The following remarkable features were found in the hypocenter distributions:

(1) A long and narrow zonal distribution of hypocenters, parallel to the trench axis, was found along the bathymetric contour of a depth of about 6 km in the outer-slope region. The focal depths of these earthquakes were found to be shallow within the upper ocean crust (layer 2 and the upper part of the layer 3). This seismic activity appears to be associated with the graben structures which develop in this region.

(2) A seismic activity occurred in clusters near the trench axis in the outer-slope region. The focal depths of these earthquakes extend from the shallow crust into the uppermost mantle almost down to about 45 km from the sea-level, forming a nearly vertical plane. This plane corresponds to the location of the main shock of the 1933 large off-Sanriku earthquake.

(3) A swarm earthquake activity occurred in the inner-slope region at the water depth of 2–3 km. The focal depths of these earthquakes are at the interface between the overlying landside rock mass and the underlying ocean crust.

The above distinct three groups of seismic activities would represent

the present-day major tectonic movements in the Japan Trench region, Northeast Japan. They are (1) a broad bending motion of the ocean crust which is associated with many graben structures in the outer-slope region, (2) a subsidence and its associated sharp bending deformation of the ocean crust under the inner-slope region, near to the trench axis, being accompanied by lithospheric fractures, (3) either a slip or a thrust faulting motion between the overlying landside rock mass and underlying ocean crust.

Acknowledgements

We express our hearty thanks to Professors N. Nasu and M. Horikoshi, the Ocean Research Institute, University of Tokyo, the chief scientists of the R/V Hakuho-Maru cruises KH-81-3 and KH-81-4, and Captain I. Tadama and the crews of the R/V Hakuho-Maru. We also thank Mr. Y. Nishi and Miss H. Sugimoto for their contributions to the improvements of the earthquake location algorithms.

This study was supported by the Grant-in-Aid for Scientific Research, Project Number 54201, 1980-1982, the Ministry of Education, Science and Culture.

References

DUSCHENS, J., R.C. LILWALL and T.J.G. FRANCIS, 1983, The hypocentral resolution of microearthquake survey carried out at sea, *Geophys. J.R. astr. Soc.*, **72**, 435-451.

ENGDAHL, E.R. and W.H.K. LEE, 1976, Relocation of local earthquakes by seismic ray tracing, *J. Geophys. Res.*, **81**, 4400-4406.

ENGDAHL, E.R., J.W. DEWEY and K. FUJITA, 1982, Earthquake location in island arcs, *Phys. Earth and Planet. Inter.*, **30**, 145-156.

FACULTY OF SCIENCE, TOHOKU UNIVERSITY, 1983, Microearthquake activity in and around the Tohoku District (November, 1982-April, 1983), *Report of Coordinating Committee for Earthquake Prediction*, **30**, 19-29.

FROHLICH, C., S. BILLINGTON, E.R. ENGDAHL and A. MALAHOFF, 1982, Detection and location of earthquakes in the Central Aleutian subduction zone using island and ocean bottom seismograph stations, *J. Geophys. Res.*, **87**, 6853-6864.

HAMILTON, E.L., 1976, Shear wave velocity versus depth in marin sediments: a review, *Geophysics*, **41**, 985-996.

HASEGAWA, A., N. UMINO and A. TAKAGI, 1978, Double-planed structure of the deep seismic zone in the northeastern Japan arc, *Tectonophysics*, **47**, 43-58.

HIRATA, N., T. YAMADA, H. SHIMAMURA, H. INATANI and K. SUYEHIRO, 1983, Spatial distribution of microearthquakes beneath the Japan Trench from ocean bottom seismographic observations, *Geophys. J.R. astr. Soc.*, **73**, 653-669.

IWABUCHI, Y., 1980, Topography of trenches in the adjacent seas of Japan, *Marine Geodesy*, **4**, 121-140.

ICHIKAWA, M., 1978a, Lateral heterogeneity under southern Kurile Trench and its vicinity and systematic discrepancy in epicenter locations, *Geophys. Mag.*, **38**, 1-19.

ICHIKAWA, M., 1978b, A new subroutine program for determination of earthquake

parameters and local travel time tables for events near the southern Kurile Trench, *Quarterly Journal of Seismology*, 43, 11-19.

ICHIKAWA, M., 1979, Determination of hypocenters of earthquakes occurring off the east coast of northern Honshu, *Quarterly Journal of Seismology*, 43, 59-65.

JACOB, K.H., 1970, Three-dimensional ray tracing in a laterally heterogeneous spherical earth, *J. Geophys. Res.*, 75, 6685-6689.

JAMES, D.E., I.S. SACKS, L.E. LAZO and G.P. APARICIO, 1969, On locating local earthquakes using small networks, *Bull. Seis. Soc. Amer.*, 59, 1201-1212.

JAPAN METEOROLOGICAL AGENCY, 1983, The seismological bulletin of the Japan Meteorological Agency for March and April.

JULIAN, B.R., and D. GUBBINS, 1977, Three-dimensional seimic ray tracing, *J. Geophys.*, 43, 95-114.

KANAMORI, H., 1971, Seismological evidence for a lithosphere normal faulting, the Sanriku earthquake of 1933, *Phys. Earth Planet. Inter.*, 4, 289-300.

KASAHARA, J., S. NAGUMO and S. KORESAWA, 1978, Seimic gap and seismotectonic structure off the coast of northern Honshu, Japan, observed by OBS, Program and Abstract, Seismol. Soc. Japan, 1978, no. 2, 43.

KASAHARA, J., S. NAGUMO, S. KORESAWA, Y. NISHI and H. SUGIMOTO, 1982, A linear trend of hypocenter distribution in the outer-slope region of the Japan Trench revealed by OBS array —preliminary report—, *Bull. Earthq. Res. Inst., Univ. Tokyo*, 57, 83-104.

LEE, W.H.K., and J.C. LAHR, 1975, HYP071 (revised), a computer program for determining hypocenter, magnitude, and first motion pattern of local earthquakes, *U.S. Geol. Survey, Open-File Report 75-311*, 113 pp.

LEE, W.H.K., and S.W. STEWART, 1981, Principles and applications of microearthquake networks, Academic Press, New York.

LILWALL, R.C., and T.J.G. FRANCIS, 1978, Hypocentral resolution of small ocean bottom seismic networks, *Geophys. J.R. astr. Soc.*, 54, 721-728.

LOMNITZ, C., 1977, A fast epicenter location program, *Bull. Seism. Soc. Amer.*, 67, 425-431.

LUDWIG, W.J., *et al.*, 1966, Sediments and structure of the Japan Trench, *J. Geophys. Res.*, 71, 2121-2137.

NAGUMO, S., S. HASEGAWA, S. KORESAWA and H. KOBAYASHI, 1970, Ocean-bottom seismographic observation off Sanriku—aftershock activity of the 1968 Tokachioki earthquake and its relation to ocean-continent boundary fault, *Bull. Earthq. Res. Inst. Univ. Tokyo*, 48, 793-809.

NAGUMO, S., J. KASAHARA and S. KORESAWA, 1976, Structure of microearthquake activity around Japan Trench, off Sanriku, obtained by ocean-bottom seismographic network observation, *J. Phys. Earth*, 24, 215-225.

NAGUMO, S., J. KASAHARA and S. KORESAWA, 1978, Shallow earthquake activity in the oceanic plate near the Erimo seamount, Program and Abstract, Seismol. Soc. Japan, 1978, No. 1, 38.

NAGUMO, S., 1980, Seismic activity and geological structure across the Japan Trench and forearc, in Zisin, eds, R. Sugiyama et al., Tokai University Press, Tokyo, 25-40.

NAGUMO, S., T. OUCHI and S. KORESAWA, 1980, Seismic velocity structure near the extinct spreading center in the Shikoku Basin, North Philippine Sea, *Marine Geology*, 35, 135-146.

NASU, N., *et al.*, 1979, Multi-channel seismic reflection data across the Japan Trench, IPOD-Japan Basic Data Series, No. 3, Ocean Res. Inst., University of Tokyo.

NISHI, Y., 1982, Hypocenter determination in the three-dimensional heterogeneous media using ray initializer, Master thesis, University of Tokyo.

OCEAN-BOTTOM SEISMOLOGY DIVISION, EARTHQ. RES. INST., UNIVERSITY OF TOKYO, 1983a,

Focal mechanism of the earthquake swarm on July 7, 1981, occurred in the inner-slope region of the Japan Trench, *Report of the Coordinating Committee for Earthquake Prediction*, **29**, 20-21.

OCEAN-BOTTOM SEISMOLOGY DIVISION, EARTHQ. RES. INST., UNIVERSITY OF TOKYO, 1983b, Focal mechanism of the linear trend earthquakes occurred in the outer-slope region of the Japan Trench, *Report of the Coordinating Committee for the Earthquake Prediction*, **29**, 22-23.

SUGIMOTO, H., 1983, Hypocenter determination of microearthquakes occurring off Sanriku, Japan Trench region—an evaluation of the focal depth determination—, Master thesis, Chiba University.

THURBER, C. H., and W. L. ELLSWORTH, 1980, Rapid solution of ray tracing problem in heterogeneous media, *Bull. Seis. Soc. Amer.*, **70**, 1137-1148.

VON HUENE, R., M. LANGSETH, N. NASU and H. OKADA, 1980, Summary, Japan Trench transect, Initial Reports, Deep Sea Drilling Project, 57 and 58, Washington (U. S. Government Printing Office), 473-488.

Appendix: List of hypocenters off Sanriku, Japan Trench region, determined by ocean-bottom seismometer array observation in June-July, 1981.

Earthq. No.	Y	Date M	D	Origin Time H	M	S	Lat. D	M	Long. D	M	Depth KM	M
5	1981	June	12	00	41	15.69	39	54.33	144	45.01	5.91R	3.2
7			13	16	29	55.42	39	15.94	144	22.68	28.21	3.4
8			13	20	03	12.72	39	16.53	144	23.57	47.29	3.5
9			14	02	26	01.65	39	38.11	144	47.12	5.91R	2.9
10			14	02	40	43.92	39	56.84	144	46.33	5.91R	2.8
12			14	15	56	46.01	39	07.18	144	27.64	36.63	3.8
13			15	01	01	31.45	39	42.50	143	03.83	29.37	3.6
14			15	08	53	03.68	39	04.29	144	27.36	24.10	3.7
16			17	03	25	33.87	39	08.88	144	17.51	31.09	3.9
17			17	23	10	45.90	39	05.91	144	22.12	5.26	3.4
18			18	09	44	27.96	39	52.17	144	49.52	8.29	2.8
19			18	11	33	41.55	39	20.48	144	27.81	6.54	3.0
20			19	21	40	53.82	39	27.53	144	43.47	6.38	2.9
21			19	23	09	39.09	38	51.73	143	16.34	44.26	3.5
22			20	00	53	48.57	39	49.17	144	41.71	5.91R	3.1
24			20	05	54	25.47	39	57.56	144	46.85	29.40	3.5
26			20	10	15	07.01	39	48.78	144	59.00	5.91R	2.8
27			21	18	52	32.11	39	15.78	144	29.24	5.90	3.2
28			22	08	57	40.11	38	39.90	144	26.01	39.63	3.8
29			23	08	34	30.92	39	17.38	144	20.00	17.56	3.5
30			23	18	19	35.35	39	43.83	144	50.24	8.93	3.2
31			23	18	22	47.50	38	57.43	144	38.16	11.12	3.3
33			24	12	11	41.49	39	17.42	144	20.73	18.71	3.8
34			25	20	40	58.51	39	37.85	144	43.74	5.91R	3.4
35			26	06	03	35.12	39	52.63	142	56.50	14.53	3.7
38			26	11	51	14.72	40	18.95	144	08.04	5.91R	3.3

Appendix: (continued)

Earthq. No.	Y	Date M	D	Origin Time H	M	S	Lat. D	M	Long. D	M	Depth KM	M
39			26	15	51	36.32	39	38.27	143	26.53	13.50	3.1
40			27	01	03	54.05	39	51.27	144	07.76	5.91R	3.9
41			27	05	44	45.10	39	08.05	144	37.01	22.85	3.2
42			27	07	13	01.30	39	31.66	144	45.89	35.80	3.7
43			29	04	19	51.53	39	12.56	144	40.18	5.91R	4.2
45			29	19	22	37.67	39	21.19	144	23.35	32.35	3.1
47			30	10	34	19.84	39	24.57	144	26.85	33.14	3.2
48			30	21	36	17.67	39	21.28	144	23.08	5.91R	3.3
49	1981	July	01	03	41	53.68	39	17.15	144	46.23	13.90	3.2
50			01	22	00	25.95	39	18.10	143	34.09	19.51	3.2
51			02	08	57	42.98	40	33.44	144	10.39	27.61	3.8
52			02	16	42	12.84	38	58.42	143	42.81	5.91R	3.4
53			02	23	16	15.99	39	17.17	144	46.39	6.03	3.3
54			02	04	01	21.11	39	31.09	144	44.43	29.81	3.6
55			03	06	26	12.23	39	03.55	144	43.58	5.91R	3.5
57			03	14	34	01.11	39	27.72	143	01.82	13.44	3.9
59			04	23	00	05.47	39	36.79	144	45.94	5.91R	2.8
60			05	04	35	29.74	39	07.09	144	23.55	25.02	3.7
63			08	03	36	59.52	39	32.36	143	17.96	14.66	3.9
88			09	10	19	46.31	39	51.82	143	41.78	10.75	5.1
67			09	10	28	47.86	39	53.67	143	40.18	11.71	5.4
68			09	10	41	47.70	39	51.85	143	39.79	12.82	4.3
69			09	10	45	13.07	39	52.28	143	39.67	12.92	4.9
89			09	11	10	24.69	39	55.66	143	38.08	8.54	4.9
71			09	13	19	37.36	39	50.75	143	36.38	10.50	3.8
72			09	14	41	28.97	39	20.69	144	29.04	22.44	3.7
73			09	17	32	50.77	39	54.51	143	40.02	10.17	3.5
74			10	00	44	00.97	39	53.69	143	38.54	14.47	4.3
75			10	13	59	42.60	40	02.84	144	36.67	6.61	3.0
76			10	18	18	54.78	39	58.55	144	41.07	3.21	3.3
80			12	02	24	54.30	39	07.35	144	22.21	33.10	3.5
83			13	14	26	09.08	39	39.60	144	48.30	5.91R	3.2

(R: Restrained)

三陸沖日本海溝域における震源分布
—海底地震計群列観測による—

地震研究所 南雲昭三郎 笠原順三 是澤定之

海底地震計群列観測を，1981年夏，三陸沖日本海溝域において行い，7観測点で，6月11日から7月12日に至る33日間の同時観測のデータを得た．群列観測網は海溝軸を挟んで海盆側と島弧側と両方に設けた．震源深度の分解能を高めるために，新しく震源決定アルゴリズムを開発した．それは (1) 3次元不均質構造を取扱う Ray Initializer を用いたこと，(2) 最小二乗法反復手順に震源発震時に対する拘束条件を加えたこと，(3) 初期試行震源深度の影響を吟味する手順を加えたことなどに特徴づけられる．その結果，日本海溝域の震源分布について，3つの群が見出された．それらの特徴は次の通りである．

(1) 1つの群は日本海溝外側斜面域において水深約 6 km の等深線に沿って，長くかつ狭い幅の線状傾向を示す帯状分布である．これらの地震の震源深度は浅く，海洋地殻内に起っている．これらは海溝外側斜面域に発達する地溝構造に対応しているようであり，海洋地殻の曲げ変形運動を表わしているものと思われる．

(2) 2つめの群は海溝軸の近傍，外側斜面下に房状のまとまりを示す地震である．その場所は1933年三陸沖大地震 (M=8.3) の主震の震央に対応している．これらの地震の震源深度は深く，海洋地殻からモホ面下，最上部マントル内部約 45 km にわたって起っており，その分布はほぼ垂直に近い面に沿っており，海洋リソスフィヤの断層運動を示しているようである．この最上部マントル内の地震活動は海溝軸を越えて海溝内側斜面下へ沈み込む海洋地殻の鋭い曲げ変形と沈降とに関連しているもののようである．

(3) 3つめの群は海溝内側斜面下水深 2-3 km の地域に起った群発地震である．これらの地震の震源深度は海洋地殻と上盤の陸側岩体との境界付近にあたっている．この地震活動は境界面に沿うすべり或は断層運動を表わしているものであろう．